J Wood Sci (2006) 52:128–133
DOI 10.1007/s10086-005-0737-4

ORIGINAL ARTICLE

Mikiji Shigematsu · Takayuki Kobayashi
Hiroyasu Taguchi · Mitsuhiko Tanahashi

Transition state leading to β-*O*′ quinonemethide intermediate of *p*-coumaryl alcohol analyzed by semi-empirical molecular orbital calculation

Received: September 24, 2004 / Accepted: May 9, 2005 / Published online: February 5, 2006

Abstract The radical coupling reaction leading to the β-*O*′ quinonemethide intermediate of *p*-coumaryl alcohol was analyzed by semi-empirical molecular orbital calculation with MOPAC2002. By analyzing the radical monomer in a one-electron oxidation, the spin density of the unpaired electron at the 4-oxygen was less than half of the values at the C_1, C_3, C_5, and C_β positions. By analyzing the transition state during the radical coupling reaction, the activation enthalpy was evaluated as 9.76 kcal/mol, which corresponds to the activation energies for the propagation of common vinyl polymers. From the analysis of atomic interactions in the transition state, it was found that the activation enthalpy was largely composed of a high coulombic repulsion between C_β of the first monomer and the phenolic oxygen of the second monomer. After passing the transition state, the two radical monomers formed a metastable quinonemethide intermediate. The optimum conformation of the quinonemethide intermediate was formed from the metastable conformation through a second transition state with a small energy barrier.

Key words Lignin · Radical coupling reaction · Transition state · Molecular orbital calculation · Activation enthalpy

Introduction

Lignin is formed by dehydrogenative polymerization (DHP) of monolignols oxidized enzymatically by the peroxidase/H_2O_2 system. The overall reaction of DHP progresses in six stages:

1. Diffusion and collision of the monolignol and enzyme in the polysaccharide matrix.
2. Penetration of monolignol into the active site of the enzyme.
3. Formation of the radical molecules by one-electron oxidation of the monolignols, and their release from the enzyme.
4. Formation of quinonemethide intermediates (generally β-*O*′, β-β′ and β-5′ linkages) with coupling reaction of the two radical monomers.
5. Stabilization of the α-carbon in the quinonemethides by the addition of a hydroxyl group for β-*O*′, resinol structure for β-β′, and coumaran structure for β-5′.
6. Further polymerization by repeating the first five stages.

In recent years, quite a number of reports on the computer simulations of lignin formation have been published. For the first stage of DHP, Houtman and Atalla[1] simulated the diffusion of monolignols near the cellulose surface, after which Houtman[2] simulated the collision of two monolignol molecules by molecular dynamics calculations. For the third stage of DHP, Kobayashi et al.[3] simulated the activity of peroxidase to monolignols and related substances by semi-empirical molecular orbital calculations. The fourth stage was addressed by Elder and Ede[4] who simulated the theoretically feasible linkages of radical coupled intermediates, and compared their reactivities by the heat of formation. For the sixth stage, Glasser and Glasser[5] simulated 100 units of lignin based on a statistical distribution of linkage types. However, the second and fifth stages of DHP have not been simulated yet. In other studies, a number of reports have emerged regarding lignin formation by examining optimum conformations of final products after stabilization (fifth stage) by molecular orbital calculation. These reports were simulated with molecular mechanics,[6] semi-empirical molecular orbital calculations,[7–9] or ab initio molecular orbital calculations.[10,11] However, these studies described the reactivity of DHP from the simulation of the stability of the final products and did not consider the reaction pathway.

M. Shigematsu (✉) · T. Kobayashi · H. Taguchi · M. Tanahashi
Faculty of Applied Biological Sciences, Gifu University, Gifu 501-1193, Japan
Tel. +81-58-293-2922; Fax +81-58-293-2922
e-mail: shige@cc.gifu-u.ac.jp

Part of this article was presented at the 46th Lignin Symposium, held in Fukuoka, October 31–November 1, 2002

Polymerization of lignin progresses through a transition state during the approach of two radical monomers (fourth stage), and the final products are formed following the formation of intermediates (fifth stage). We have focused on the former reaction, which determines the linkage types between two monomers. To search for a feasible pathway leading to coupled intermediates, the reverse reaction from coupled to uncoupled monolignols was computed. To simplify the calculation, *p*-coumaryl alcohol was selected as the model substance for monolignol, although it is an oversimplification of lignin structure. The reason for the selection was the lack of conformationally complicated methoxyl groups,[12,13] which are present in coniferyl and sinapyl alcohols (constituents of common lignin). Furthermore, modeling of the coupling reaction was limited to formation of the *β-O′* linkage, which is the main linkage type of native lignin. All modeling was conducted by semi-empirical molecular orbital calculations rather than by ab initio methods due to the less demanding computer requirements for semiempirical methods.

Methods

Computation was carried out using WinMOPAC Ver. 3.5.1a (distributed by Fujitsu). This software combined a graphical user interface for the development of the Z-matrix and MOPAC2002 Ver. 1.00 as the calculating engine.[14] The eigenvector following (EF) routine was used as the optimizer, and the gradient normal (GNORM) was set to 0.01. The Parametric Method 5 (PM5) was used to calculate the heat of formation (H_f). The unrestricted Hartree-Fock Hamiltonian approximation (UHF) was used for the monolignol radical and the coupling reaction due to the presence of an unpaired electron. For other parameters, default values programmed in MOPAC2002 were used.

The calculations proceeded as follows:

1. Full optimization of *p*-coumaryl alcohol radical by taking into consideration the geometry of the alcohol hydroxyl group, which rotates freely. All bond lengths, angles, and torsions were optimized in the computation.
2. Confirmation of the reactive atoms in the radical molecule by the localization of the unpaired electron estimated by the calculated spin density.
3. A search for the conformers of *β-O′*-linked quinonemethide intermediate by considering the geometries of C_1-C_α, C_α-C_β, C_β-$O_{4'}$, $O_{4'}$-$C_{4'}$, and $C_{1'}$-$C_{\alpha'}$ bonds, and two alcohol hydroxyl groups.
4. A search for the transition state candidates in the coupling reaction by disconnecting the *β-O′* bond in the conformers of the quinonemethide intermediate. All bond lengths, angles, and torsions except the disconnected bond length were optimized in the computation. The candidates were determined from the conformation giving maximal H_f in each diagram of atomic distance and H_f.
5. Full optimization of the transition states (TS) from the Cartesian coordinate geometries of candidates as an initial structure. Confirmation of obtained TS structures was done by a force calculation (FORCE) and an intrinsic reaction coordinates calculation (IRC). The global TS structure in *β-O′* coupling was determined as the one having the smallest energy of all TS structures.
6. Analysis of atomic interaction at the transition state by energy partitioning (ENPART).

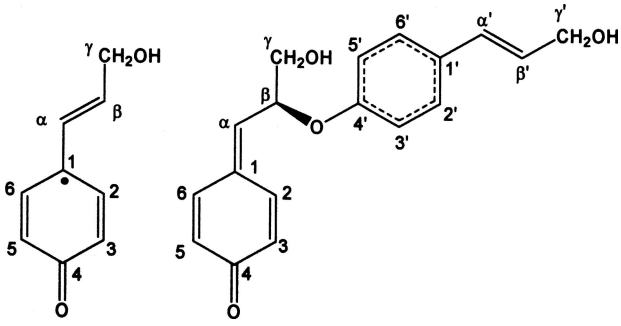

Fig. 1. Carbon numbers in *p*-coumaryl alcohol radical (*left*), and quinonemethide intermediate of (*S*-)*β-O′*-linked *p*-coumaryl alcohols (*right*)

The carbon numbers in the molecules appearing in this report are defined as shown in Fig. 1. The definition of torsion angles, i.e., the relative positions of atoms, is presented in the text.

The probability of minimum energy conformations was calculated by Boltzman's distribution. The relative probability (p) was obtained from Eq. 1:

$$p = e^{-\left(H_f - H_f^0\right)/RT} \quad (1)$$

where R is the gas constant ($1.98\,\mathrm{cal\,K^{-1}\,mol^{-1}}$), T is the absolute temperature (298 K in this report), and H_f^0 is the lowest H_f value.

Results and discussion

Optimum conformation and reactive positions of *p*-coumaryl alcohol radical

For optimum conformations of *p*-coumaryl alcohol radical, four minimum energy conformers were obtained. The optimum values of torsions and the geometries are shown in Table 1 and Fig. 2. Conformers **a′** and **b′** are symmetrical to **a** and **b**, respectively. The geometrical difference appeared in only the alcohol hydroxyl group, and the other geometries were almost identical. The energy difference between **a** and **b** was small and corresponded to 1 : 0.385 of the existing probability. The lowest H_f for the *p*-coumaryl alcohol radical was –36.76 kcal/mol. Therefore, H_f of the uncoupled state, i.e., two infinitely separated molecules, was evaluated as –73.52 kcal/mol (twice the value for a single molecule). This corresponds to the initial state of the radical coupling reaction.

The reactive positions of the *p*-coumaryl alcohol radical were analyzed from the spin population and atomic charge.

Table 1. Optimum conformations of *p*-coumaryl alcohol radical

Conformation	O_γ-C_γ-C_β-C_α (degree)	H-O_γ-C_γ-C_β (degree)	H_f (kcal/mol)	*p*
a	24.6	60.6	–36.76	1
a′	–24.6	–60.6	–36.76	1
b	156.6	–62.9	–36.20	0.385
b′	–156.6	62.9	–36.20	0.385

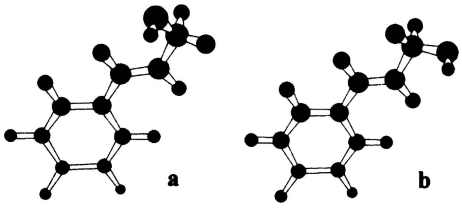

Fig. 2. Geometries of *p*-coumaryl alcohol radical optimized by UHF/PM5 protocol. Conformations correspond to those in Table 1. Conformations **a′** and **b′** are symmetries of **a** and **b**, respectively

Table 2 shows the spin populations of α-spin and β-spin, the electron density, the spin density, and the Mulliken charge for conformer **a** of the *p*-coumaryl alcohol radical. The spin density was found to be high at C_1, C_3, C_5, C_β, and O_4 suggesting the localization of an unpaired electron at these atoms, and implying the occurrence of radical coupling reaction. The atoms having high spin densities were similar to the coniferyl alcohol radical.[9,15] Additionally, the reactive atoms were negatively charged, suggesting that the radical coupling reaction proceeds despite the coulombic repulsion.

Figure 3 shows the distributions of the unpaired electron in *p*-coumaryl alcohol radical and the relative ratios predicted from the spin densities at C_1, C_3, C_5, C_β, and O_4. By assuming the coupling reaction occurs in accordance with these ratios, the radical coupling appears to occur predominantly at C_1, which has the highest spin density. However, coupling at C_1 would be difficult due to steric hindrance. Other couplings, β-β' and β-5′ may easily occur due to the high ratios at C_5 and C_β. The formation of β-O' coupling may be comparatively difficult due to the low ratio at O_4.

Unfortunately, semi-empirical molecular orbital calculation for the unpaired electron is less reliable than advanced methods including electron correlation theory, e.g., the density functional models, the Møller-Plesset models, and more advanced methods. The details of comparisons between different monolignols and between different couplings will be discussed in subsequent reports.

Conformations of quinonemethide intermediate

In the β-O' quinonemethide intermediate, many conformations are possible due to the rotation at the C_1-C_α, C_α-C_β, C_β-$O_{4'}$, $O_{4'}$-$C_{4'}$, and $C_{1'}$-$C_{\alpha'}$ bonds, and the two alcohol hydroxyl groups. Thus, the following steps were taken to arrive at the minimum energy conformations. *S*- and *R*-form enantiomers at the chiral center C_β are present in the β-O'-coupled intermediate. But as MOPAC cannot analyze the difference between the enantiomers, only the *S*-form was analyzed in this study. For the C_1-C_α bond, the position of C_β ($\phi_{\beta\text{-}\alpha\text{-}1\text{-}2}$) is considered to be mostly in the same plane as the first monomer's aromatic ring due to the presence of a double bond at C_1-C_α. For the C_α-C_β bond, the position of C_γ ($\phi_{\gamma\text{-}\beta\text{-}\alpha\text{-}1}$) is considered to be anti to C_1 due to the monomer structure. Simultaneously, the position of $O_{4'}$ is restricted by the position of C_γ due to the sp^3 orbital of C_β. For the C_β-$O_{4'}$ bond, the position of $C_{4'}$ can be defined as the torsion angle against C_α ($\phi_{4'\text{-}O'\text{-}\beta\text{-}\alpha}$), and would be restricted at three *gauche* positions against C_α, C_γ, and H_β. For the $O_{4'}$-$C_{4'}$ bond, the aromatic ring of the second monomer is mostly restricted to be parallel to the aromatic ring (first monomer)-C_α-C_β plane by steric hindrance. For $C_{1'}$-$C_{\alpha'}$, $C_{\beta'}$ is limited to two positions against the aromatic plane of the second monomer (definable as $\phi_{3'\text{-}4'\text{-}O'\text{-}\beta}$) analogous with the conformation of the monomer. In addition, four geometries of the alcohol hydroxyl group (**a**, **a′**, **b**, and **b′**) shown in the monomer structure must be considered for each monomer. These 96 possible conformers ($1\times1\times3\times1\times2\times4\times4$) were used as the initial structure for full optimization. In addition, the feasible transition states were derived by disconnecting the β-O' bond from all optimum conformers of quinonemethide intermediate. Table 3 shows the low H_f conformations of the quinonemethide intermediate of (*S*-)β-O'-linked *p*-coumaryl alcohols, as well as the low energy transition states. Typical examples of the geometries, **QM1** and **TS1**, are shown in Fig. 4.

In low energy conformers of the quinonemethide intermediate (**QM1**-**8**), the positions of $C_{4'}$ were similar and anti to H_β in the $O_{4'}$-C_β bond. Furthermore, rotation of the second monomer's aromatic ring at the $C_{4'}$-$O_{4'}$ bond was restricted within the range of 70°–90°; the absolute value in $C_{3'}$ shows the torsion of the two aromatic planes, and the sign shows the direction of $C_{\beta'}$. The γ-hydroxymethyl group was restricted by **a** and **b** forms but not **a′** and **b′** (see $O_\gamma H_\gamma$). These conformational restrictions could possibly be due to the united effects of hydrogen bonding and steric hindrance between the hydroxyl group and the aromatic ring. The influence of the $C_{\beta'}$ position on H_f was minimal because of the appearance of both positive and negative signs of $C_{3'}$ in Table 3. Furthermore, the γ'-hydroxymethyl group was restricted to **a** and **a′** forms (see $O_{\gamma'}H_{\gamma'}$), which are optimum conformations that are analogous to the results of the radical monomers shown in Table 1. These results suggest negligible atomic interactions with the first monomer's atoms due to their distance of separation.

Table 2. Spin population and charge density of each atom in conformer **a** of *p*-coumaryl alcohol radical computed by UHF/PM5 protocol

Atom	Spin population				Mulliken atomic charge
	α-spin	β-spin	Electron density	Spin density	
C_1	2.342	1.673	4.015	0.669	–0.015
C_2	1.825	2.294	4.119	–0.469	–0.119
C_3	2.398	1.849	4.247	0.549	–0.247
C_4	1.741	1.912	3.653	–0.170	0.347
C_5	2.394	1.854	4.247	0.540	–0.247
C_6	1.826	2.293	4.119	–0.467	–0.119
C_α	1.824	2.309	4.132	–0.485	–0.132
C_β	2.417	1.826	4.244	0.591	–0.244
C_γ	1.978	2.033	4.011	–0.054	–0.011
O_γ	3.214	3.210	6.424	0.004	–0.424
O_4	3.323	3.048	6.371	0.274	–0.371
H_2	0.431	0.404	0.835	0.028	0.165
H_3	0.386	0.420	0.805	–0.034	0.195
H_5	0.385	0.419	0.804	–0.034	0.196
H_6	0.429	0.402	0.830	0.027	0.170
H_α	0.429	0.400	0.829	0.029	0.171
H_β	0.400	0.435	0.834	–0.035	0.166
H_γ	0.436	0.413	0.849	0.023	0.151
H_γ	0.456	0.443	0.898	0.013	0.102
H_O	0.365	0.365	0.731	0.000	0.269
Total	29.000	28.000	57.000	1.000	0.000

Electron density: sum of α-spin and β-spin.; spin density: excess of α-spin over β-spin

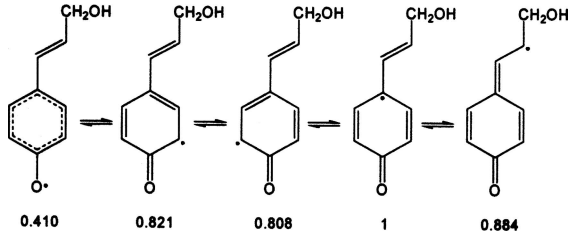

Fig. 3. Distribution of unpaired electron in *p*-coumaryl alcohol radical. The values indicate the relative ratios predicted from the spin densities at C_1, C_3, C_5, C_β, and O_4

Conformations and intermolecular interactions between radical monomers at the transition state

In the low energy conformations of the transition state (**TS1**-**8**) shown in Table 3, the positions of $O_{4'}$ are similar; the C_β-$O_{4'}$ distances were about 1.93 Å, and the $O_{4'}$-C_β-C_α bond angles were about 100° for all transition states. These similarities would be governed quantum mechanically by the sp^3 orbital of C_β and $O_{4'}$. In these transition states, the positions of $C_{4'}$ of the second monomer were similar, and restricted to be anti to C_γ. The structural difference between these transition states and coupled intermediates may be due to the strong hydrogen bonding of the γ-hydroxyl group to $O_{4'}$ of the first monomer, and the small interaction with π-electrons in the second monomer's incomplete aromatic ring.

For the lowest energy conformation (**TS1**), only one imaginary vibrational frequency was obtained at $-649.88\,cm^{-1}$ in the direction of approach of C_β and $O_{4'}$. This conformation was verified as the transition state because only one imaginary frequency was obtained. Also, with the direction indicating the approach of C_β and $O_{4'}$, this transition state was verified to be reactive toward the *β-O′* linkage. The activation enthalpy (H_a) was calculated as 9.76 kcal/mol by using the equation $H_a = H_f(\mathbf{TS1}) - 73.52$. This value corresponds to the activation energies of radical polymerization of common vinyl polymers, e.g.,

Table 3. The major conformers extracted from 96 initial structures of quinonemethide intermediate of (*S*-)*β-O′* linked *p*-coumaryl alcohols (**QM1**-**8**) and transition states toward quinonemethide intermediate (**TS1**-**8**)

No.	Conformation					H_f (kcal/mol)	*p*
	$C_{4'}$[a]	$C_{3'}$[b]	$O_\gamma H_\gamma$[c]	$O_{\gamma'} H_{\gamma'}$[c]	*d*[d]		
QM1	H_β	73.3	**a**	**a′**	1.414	–89.33	1
QM2	H_β	73.5	**a**	**a**	1.414	–89.33	0.993
QM3	H_β	–112.0	**a**	**a′**	1.414	–89.27	0.905
QM4	H_β	–112.1	**a**	**a**	1.414	–89.27	0.901
QM5	H_β	88.9	**b**	**a**	1.416	–88.89	0.479
QM6	H_β	89.3	**b**	**a′**	1.416	–88.88	0.465
QM7	H_β	–97.0	**b**	**a**	1.416	–88.85	0.442
QM8	H_β	–96.8	**b**	**a′**	1.416	–88.84	0.438
TS1	C_γ	–88.1	**a**	**a′**	1.931	–63.76	1
TS2	C_γ	–90.3	**a**	**a**	1.935	–63.76	0.995
TS3	C_γ	92.6	**a**	**a**	1.930	–63.63	0.800
TS4	C_γ	–93.1	**b**	**a**	1.936	–63.40	0.537
TS5	C_γ	–93.0	**b**	**a′**	1.933	–63.34	0.491
TS6	C_γ	–87.6	**a**	**b′**	1.931	–63.33	0.484
TS7	C_γ	89.9	**a**	**a′**	1.934	–63.32	0.473
TS8	C_γ	87.0	**b**	**a**	1.931	–63.21	0.391

[a] *Anti*-atom of $C_{4'}$ with C_β-$O_{4'}$ bond
[b] Torsion angle of $C_{3'}$-$C_{4'}$-$O_{4'}$-C_β
[c] Corresponding to the conformation name of monomer shown in Table 1
[d] Distance between C_β and $O_{4'}$ in angstroms

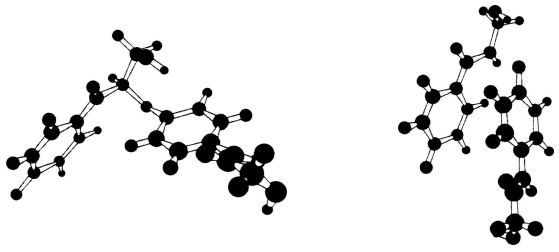

Fig. 4. Typical examples for geometries of the quinonemethide intermediate of (*S*-)*β*-*O*′-linked *p*-coumaryl alcohols (*left*, **QM1**) and the transition states during radical coupling reaction (*right*, **TS1**)

Table 4. The major intermolecular interactions between radical monomers at **TS1**

Atoms		*J* (eV)	*K* (eV)	*C* (eV)	*J* + *K* + *C* (eV)
C_β	$O_{4'}$	–2.7221	–0.9262	1.4445	–2.2038
H_O	$O_{4'}$	–0.0424	–0.0045	–0.5444	–0.5914
C_4	$O_{\gamma'}$	0.0000	0.0000	–0.3496	–0.3496
C_4	$O_{4'}$	0.0000	–0.0006	–0.3344	–0.3351
O_4	$H_{O'}$	0.0000	0.0000	–0.3198	–0.3198
H_α	$O_{4'}$	–0.0058	–0.0010	–0.2905	–0.2973
O_γ	$C_{4'}$	–0.0004	–0.0011	–0.2891	–0.2906
C_3	$O_{\gamma'}$	0.0000	0.0000	0.2509	0.2509
O_4	$C_{\beta'}$	0.0000	–0.0001	0.2574	0.2574
C_4	$H_{O'}$	0.0000	0.0000	0.2655	0.2655
C_3	$O_{4'}$	–0.0001	–0.0016	0.2674	0.2657
O_4	$O_{4'}$	0.0000	–0.0008	0.2895	0.2887
C_α	$O_{4'}$	0.0301	–0.0461	0.3894	0.3734
O_4	$O_{\gamma'}$	0.0000	0.0000	0.4034	0.4034
O_γ	$O_{4'}$	0.0044	–0.0033	0.6922	0.6933

Negative and positive values mean attractive and repulsive interactions, respectively

J, Resonance energy; *K*, exchange energy; *C*, coulombic interaction

7–8 kcal/mol for the propagation of polystyrene,[16] and is much lower than the activation energies of the decomposition of common initiators, e.g., 26–34 kcal/mol for 2,2′-azo-bis-isobutyronitrile and benzoyl peroxide. The entropy term may be assumed to be negligible, in which case the radical coupling reaction of lignin will be as fast as the propagation of vinyl polymers.

The major intermolecular atomic interactions in **TS1** were calculated and the results are shown in Table 4. The largest total interaction was, of course, that at C_β-$O_{4'}$ with –2.2038 eV of attraction. This atomic interaction contained large coulombic repulsion component caused by the negative charges of both C_β and $C_{4'}$. The excess attraction of resonance and exchange energies were caused by the approach of the two atoms having high spin densities. For other atomic pairs, the total interactions were lower than 1/3 of that of C_β-$O_{4'}$, and mostly due to coulombic interaction including hydrogen bonding. Additionally, this analysis revealed that the alcohol hydroxyl group contributes considerably to the optimum conformation of the transition state. In other words, the kind of substituent at C_γ of monomers may affect the coupling reaction, e.g., carboxyl or aldehyde groups.

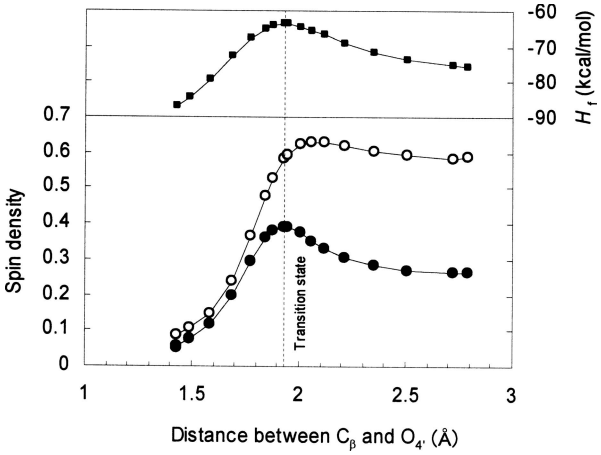

Fig. 5. The heat of formation (*filled squares*) and the spin densities at C_β (*open circles*) and $O_{4'}$ (*filled circles*) during radical coupling reaction of *p*-coumaryl alcohols as a function of the C_β-$C_{4'}$ distance

Figure 5 shows the changes of H_f and spin densities at C_β and $C_{4'}$ as functions of the atomic distance between them; this diagram was drawn by replotting the geometrical and orbital data on the reaction coordinate computed by IRC for the structure of **TS1**. In the coupling reaction, H_f values increased as the two monomers approached each other, and reached a maximum at the transition state. During the approach of the two monomers, both spin densities increased, especially at $O_{4'}$, indicating that the localization of both unpaired electrons changed due to the resonance of C_β and $O_{4'}$. The variation of spin densities during the reaction means that the radical coupling reaction cannot be expressed by only the spin density in the isolated monomer given in Table 2. After passing the transition state, H_f decreased and reached the value of the quinonemethide coupled form ($\mathbf{QM_{TS1}}$), –89.33 kcal/mol. Because H_f of $\mathbf{QM_{TS1}}$ is lower than that of the uncoupled state, it is obvious that this reaction can proceed. Simultaneously, the spin densities suddenly decreased and finally disappeared in the coupled state. Consequently, it was found that the two monomers formed the coupled state, $\mathbf{QM_{TS1}}$, by IRC analysis.

Transition from $\mathbf{QM_{TS1}}$ to **QM1**

The coupled state, $\mathbf{QM_{TS1}}$, is metastable and different from the lowest energy conformer of quinonemethide, **QM1**. $\mathbf{QM_{TS1}}$ and **QM1** were structurally different at the $C_{4'}$ position, but not at $C_{3'}$. Thus, the energy barrier in transition from $\mathbf{QM_{TS1}}$ to **QM1** with rotation of the aromatic ring of the second monomer at the C_β-$O_{4'}$ bond was analyzed. Because the analysis could not be achieved by UHF protocol, it was performed by the restricted Hartree-Fock protocol in this study. Estimated values of H_f were –87.27 kcal/mol (–88.01 kcal/mol by UHF) for $\mathbf{QM_{TS1}}$, –88.49 kcal/mol (–89.33 kcal/mol by UHF) for **QM1**, and –86.69 kcal/mol for the transition state between them. Therefore, H_a for the transition from $\mathbf{QM_{TS1}}$ to **QM1** was estimated as

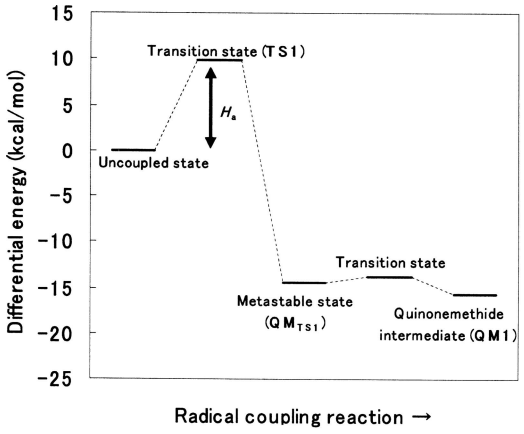

Fig. 6. Overall energy change in radical coupling reaction of two *p*-coumaryl alcohols toward *β-O′* quinonemethide intermediate. The vertical axis is the energy difference from the heat of formation of two uncoupled monomers

0.58 kcal/mol. The extremely small energy barrier indicates that this transition easily progresses.

The existence of different conformations between estimates from the transition state and the optimized quinonemethide is important for analysis of the overall reaction. This means that the thermodynamic and kinetic estimations may lead to different results. In other words, the prediction of the reactivity based on only the conformation of products is insufficient.

The overall radical coupling reaction of *p*-coumaryl alcohol leading to *β-O′*-quininemethide intermediate

Figure 6 shows the overall radical coupling reaction of *p*-coumaryl alcohol. The energy level based on the two uncoupled monomers (twice the value of conformer **a**) decreased to –15.81 kcal/mol at **QM1**. During this process, two transition states were detected by the molecular orbital calculation. One was the transition state in coupling the two monomers with H_a = 9.76 kcal/mol. The other transition state was the conformation change from the metastable quinonemethide to the optimum state. However, the energy barrier of the second transition was extremely low. Thus, the rate-determining step in the radical coupling reaction was considered to be the first reaction, i.e., bond formation between C_β and $C_{4'}$. It is concluded that the radical coupling reaction occurs by kinetic control.

Acknowledgments This study was supported by Grants-in-Aid (Nos. 11760120 and 15580143) from the Ministry of Education, Culture, Sports, Science and Technology of Japan. The authors thank Dr. Sachi Sri Kantha and Dr. Siaw Onwona-Agyeman, Gifu University, for their help in preparation of the manuscript.

References

1. Houtman CJ, Atalla RH (1995) Cellulose-lignin interactions. A computational study. Plant Physiol 107:977–984
2. Houtman CJ (1999) What factors control dimerization of coniferyl alcohol? Holzforschung 53:585–589
3. Kobayashi T, Suzuki M, Taguchi H, Shigematsu M, Tanahashi M (2001) Analysis of rate-determining factors in the oxidative reaction of monolignols by peroxidase–H_2O_2 system. Jpn Chem Program Exchange J 13:183–186
4. Elder T, Ede RM (1995) Coupling of coniferyl alcohol in the formation of dilignols. A molecular orbital study. Proceedings of the 8th International Conference on Wood and Pulping Chemistry, Helsinki, vol 1, pp 115–122
5. Glasser WG, Glasser HR (1974) Simulation of reactions with lignin by computer (SIMREL). I. Polymerization of coniferyl alcohol monomers. Macromolecules 7:17–27
6. Simon JP, Eriksson K-EL (1995) A molecular mechanics investigation of lignin structure. I. Conformational analysis of 1-phenyl-2-phenoxy-1,3-propanediol using MM3. Holzforschung 49:429–438
7. Gravitis J, Erins P (1983) Topological and conformational structure and macroscopic behavior of lignin. J Appl Polym Sci Appl Polym Symp 37:421–440
8. Elder TJ, McKee ML, Worley SD (1988) The application of molecular orbital calculations to wood chemistry. V. The formation and reactivity of quinone methide intermediates. Holzforschung 42:233–240
9. Russell WR, Forrester AR, Chesson A, Burkitt MJ (1996) Oxidative coupling during lignin polymerization is determined by unpaired electron delocalization within parent phenylpropanoid radicals. Arch Biochem Biophys 332:357–366
10. Simon JP, Eriksson K-EL (1996) The significance of intramolecular hydrogen bonding in the *β-O*-4 linkage of lignin. J Mol Struct 384:1–7
11. Simon JP, Eriksson K-EL (1998) Computational studies of the three-dimensional structure of guaiacyl *β-O*-4 lignin models. Holzforschung 52:287–296
12. Shigematsu M, Kobayashi T, Tanahashi M (2001) Solvent effect on the conformations of phenol, anisole and guaiacol simulated with MOPAC2000. Jpn Chem Program Exchange J 13:177–182
13. Shigematsu M, Kobayashi T, Yoshitani K, Tanahashi M (2002) Solvent effect on the conformation of 2,6-dimethoxyphenol simulated with MOPAC2000. J Comput Chem Jpn 1:129–134
14. Stewart JJP (2001) MOPAC2002. Fujitsu, Tokyo, Japan
15. Elder TJ, Worley SD (1984) The application of molecular orbital calculations to wood chemistry. The dehydrogenation of coniferyl alcohol. Wood Sci Technol 18:307–315
16. Brandrup J, Immergut EH (1989) Polymer handbook, 3rd edn. Wiley, New York